

# Enhancement of Redox Stability and Electrochromic Performance of Aromatic Polyamides by Incorporation of (3,6-Dimethoxycarbazol-9-yl)-triphenylamine Units

Hui-Min Wang, Sheng-Huei Hsiao

Department of Chemical Engineering and Biotechnology, National Taipei University of Technology, Taipei 10618, Taiwan

Correspondence to: S.-H. Hsiao (E-mail: shhsiao@ntut.edu.tw)

Received 18 September 2013; accepted 24 October 2013; published online 25 November 2013

DOI: 10.1002/pola.27001

**ABSTRACT:** New series aromatic polyamides with (carbazol-9-yl) triphenylamine units were synthesized from a newly synthesized diamine monomer, 4,4'-diamino-4''-(3,6-dimethoxycarbazol-9-yl) triphenylamine, and aromatic dicarboxylic acids via the phosphorylation polyamidation technique. These polyamides exhibit good solubility in many organic solvents and can be solution-cast into flexible and strong films with high thermal stability. They show well-defined and reversible redox couples during oxidative scanning, with a strong color change from colorless neutral form to yellowish green and blue ox-

dized forms at applied potentials scanning from 0.0 to 1.3 V. They show enhanced redox-stability and electrochromic performance as compared to the corresponding analogs without methoxy substituents on the active sites of the carbazole unit. © 2013 Wiley Periodicals, Inc. *J. Polym. Sci., Part A: Polym. Chem.* **2014**, 52, 272–286

**KEYWORDS:** carbazole; electrochemistry; electrochromic polymers; polyamides; redox polymers; spectroelectrochemistry; triphenylamine

**INTRODUCTION** Electrochromism refers to the reversible electromagnetic absorbance/transmittance and color change resulting from the oxidation or the reduction of the material in response to an externally applied potential by electrochemical means.<sup>1</sup> One of the main uses of electrochromic materials is in smart windows for cars and buildings and in antiglare rear-view mirrors.<sup>2</sup> Potential applications in information storage,<sup>3</sup> electrochromic displays,<sup>4</sup> and adaptive camouflages<sup>5</sup> can also be envisioned. Among the different types of electrochromic materials, conjugated polymers<sup>6</sup> such as polyanilines, polypyrroles, polyselenophenes, polythiophenes, and in particular, poly(3,4-ethylenedioxythiophene) and its derivatives<sup>7</sup> attract great interest because of mechanical flexibility, ease in band-gap/color-tuning via structural control, and the potential for low-cost processing for large-area devices. For efficient operation of an electrochromic device, it is necessary to take a number of properties into consideration: electrochromic efficiency, optical contrast, response time, stability, and durability. The difficulty in achieving satisfactory values for all these parameters at the same time stimulates the development of new methods of preparation of electrochromic films, new materials, and components for the devices.<sup>8</sup>

Because of the fact that triarylamines play an important role as hole conducting species in optoelectronic devices<sup>9</sup> and for electrochromic applications,<sup>10</sup> numerous investigations have

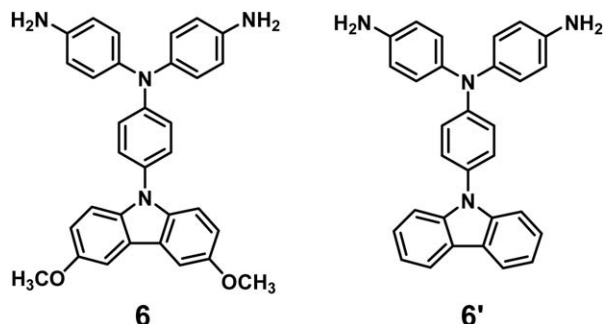
been devoted to their synthesis and the investigation of their electronic, optical, and materials properties.<sup>11</sup> The widespread use of triarylamines has its origin in the high stability of the corresponding radical cations, that is, triarylamines can reversibly be oxidized as long as the *para*-position of the phenyl rings is protected.<sup>12</sup> Electron-rich triarylamines can be easily oxidized to form stable radical cations, and the oxidation process is always associated with a noticeable change of coloration. Thus, several triarylamine-based polymers have been investigated for electrochromic applications.<sup>10</sup> In recent years, triarylamine-based condensation-type polymers such as aromatic polyamides and polyimides have been reported as a new and attractive family of electrochromic materials because of high electroactivity of the triarylamine unit and high thermal stability of the polymer backbone.<sup>13,14</sup> It has also been reported in our previous publications<sup>15</sup> that the incorporation of electron-donating or bulky substituents such as methoxy or *t*-butyl groups at the *para*-position of phenyl rings of the triphenylamine (TPA) unit resulted in stable TPA cationic radicals and decreased oxidation potential, leading to a significant enhancement on redox and electrochromic stability of the prepared polyamides.

In recent years, carbazole derivatives have been widely used as effective host materials in phosphorescent light-emitting diodes because of their sufficiently high triplet energy and

Additional Supporting Information may be found in the online version of this article.

© 2013 Wiley Periodicals, Inc.

good hole-transporting ability.<sup>16</sup> Carbazole can be easily functionalized at its (3,6-), (2,7-), or *N*-positions, and then covalently linked into polymeric systems, both in the main chain as building blocks and in a side chain as subunit.<sup>17</sup> Carbazole-containing polymers are considered as a very important class of electroactive and photoactive materials because of their unique properties, which allow various optoelectronic applications such as photoconductive, electroluminescent, electrochromic and photorefractive materials.<sup>18</sup> In a previous publication,<sup>19</sup> Liou's group studied the preparation and properties of a series of polyamides bearing (carbazol-9-yl)triphenylamine (CzTPA) units from the diamine monomer 4,4'-diamino-4''-(carbazol-9-yl)triphenylamine (**6'**) and various dicarboxylic acids. The polyamides reveal good redox stability during the first oxidation process, which is associated with a noticeable change of the coloration. However, the second oxidation process of these polymers is not reversible, possibly due to the electrochemical coupling of carbazoles through the active C-3 and C-6 sites. In this work, we synthesized a new CzTPA-based diamine monomer, 4,4'-diamino-4''-(3,6-dimethoxycarbazol-9-yl)triphenylamine (**6**), and its derived aromatic polyamides with main-chain TPA and pendent 3,6-dimethoxycarbazole units. The incorporation of electron-donating methoxy substituents on the active sites of the pendent carbazoles is expected to increase the electrochemical and electrochromic stability of the resulting polyamides. For a comparative study, some properties of the present polyamides are compared with those of structurally related ones based on the parent CzTPA-diamine monomer **6'**.



## EXPERIMENTAL

### Monomer Synthesis

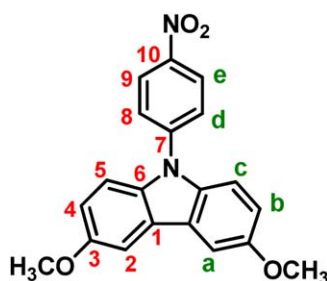
According to a reported procedure,<sup>20</sup> 3,6-dibromo-9*H*-carbazole (**1**) was prepared from the bromination of carbazole with *N*-bromosuccinimide (NBS). Following a procedure published in literature,<sup>21</sup> synthesis of 3,6-dimethoxycarbazole (**2**) was achieved by direct methoxide displacement of bromine from **1** by using sodium methoxide (MeONa) and CuI in DMF. The synthetic details and characterization data of compounds **1** and **2** are included in the Supporting Information.

### 3,6-Dimethoxy-9-(4-nitrophenyl)carbazole (**3**)

In a 250-mL one-neck round-bottomed flask equipped with a stirring bar, a mixture of 9.0 g (0.04 mol) of 3,6-dimethoxycarbazole, 5.6 g (0.04 mol) of 4-fluoronitrobenzene, and 6.1 g (0.04 mmol) of cesium fluoride (CsF) in 40 mL of dimethyl

sulfoxide (DMSO) was heated at 140 °C for 18 h under a nitrogen atmosphere. The mixture was poured into 200 mL of methanol, and the precipitated compound was collected by filtration and washed thoroughly by methanol and hot water. The crude product was filtered and recrystallized from DMF/methanol to afford 5.6 g (80% in yield) of orange crystals with a mp of 217–219 °C (by DSC at a scan rate of 2 °C min<sup>-1</sup>). FTIR (KBr): 1325, 1595 cm<sup>-1</sup> (–NO<sub>2</sub> stretch).

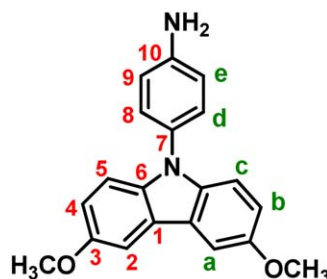
<sup>1</sup>H NMR (500 MHz, DMSO-*d*<sub>6</sub>,  $\delta$ , ppm): 3.89 (s, 6H, –OCH<sub>3</sub>), 7.07 (dd, *J* = 9.0, 2.0 Hz, 2H, H<sub>b</sub>), 7.50 (d, *J* = 9.0 Hz, 2H, H<sub>c</sub>), 7.85 (d, *J* = 2.0 Hz, 2H, H<sub>a</sub>), 7.91 (d, *J* = 8.9 Hz, 2H, H<sub>d</sub>), 8.46 (d, *J* = 8.9 Hz, 2H, H<sub>e</sub>). <sup>13</sup>C NMR (125 MHz, DMSO-*d*<sub>6</sub>,  $\delta$ , ppm): 55.62 (–OCH<sub>3</sub>), 103.55 (C<sup>2</sup>), 110.85 (C<sup>5</sup>), 115.38 (C<sup>4</sup>), 124.32 (C<sup>1</sup>), 125.52 (C<sup>9</sup>), 125.82 (C<sup>8</sup>), 134.16 (C<sup>6</sup>), 143.47 (C<sup>10</sup>), 144.55 (C<sup>7</sup>), 154.45 (C<sup>3</sup>).



### 3,6-Dimethoxy-9-(4-aminophenyl)carbazole (**4**)

In a 250-mL three-neck round-bottomed flask equipped with a stirring bar, 7.0 g (0.02 mol) of compound **3** and 0.15 g of 10% Pd/C were dissolved/suspended in 160 mL of ethanol. The suspension solution was heated to reflux under a nitrogen atmosphere, and 3 mL of hydrazine monohydrate was added slowly to the mixture, then the solution was stirred at reflux temperature. After a further 16 h of reflux, the solution was filtered to remove Pd/C, and the filtrate was cooled under a nitrogen atmosphere to grow colorless crystals. The products were collected by filtration and dried *in vacuo* at 80 °C; yield = 4.2 g (66%), mp = 131–134 °C (by DSC at 2 °C min<sup>-1</sup>). FTIR (KBr): 3350, 3465 cm<sup>-1</sup> (–NH<sub>2</sub> stretch).

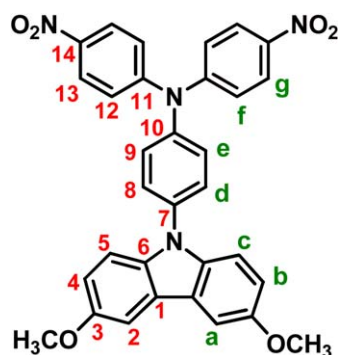
<sup>1</sup>H NMR (500 MHz, DMSO-*d*<sub>6</sub>,  $\delta$ , ppm): 3.87 (s, 6H, –OCH<sub>3</sub>), 5.37 (s, 2H, –NH<sub>2</sub>), 6.79 (d, *J* = 8.6 Hz, 2H, H<sub>e</sub>), 7.01 (dd, *J* = 9.0, 2.0 Hz, 2H, H<sub>b</sub>), 7.15 (d, *J* = 8.6 Hz, 2H, H<sub>d</sub>), 7.16 (d, *J* = 9.0 Hz, 2H, H<sub>c</sub>), 7.77 (d, *J* = 2.0 Hz, 2H, H<sub>a</sub>). <sup>13</sup>C NMR (125 MHz, DMSO-*d*<sub>6</sub>,  $\delta$ , ppm): 55.60 (–OCH<sub>3</sub>), 103.08 (C<sup>2</sup>), 110.29 (C<sup>5</sup>), 114.57 (C<sup>9</sup>), 115.01 (C<sup>4</sup>), 122.47 (C<sup>1</sup>), 125.12 (C<sup>7</sup>), 127.28 (C<sup>8</sup>), 136.23 (C<sup>6</sup>), 148.07 (C<sup>10</sup>), 153.19 (C<sup>3</sup>).



**4,4'-Dinitro-4''-(3,6-dimethoxycarbazol-9-yl)triphenylamine (5)**

In a 250-mL one-neck round-bottomed flask equipped with a stirring bar, a mixture of 6.36 g (0.02 mol) of compound **4**, 5.7 g (0.02 mol) of 4-fluoronitrobenzene, and 6.1 g (0.02 mol) of CsF in 70 mL of DMSO was heated at 140 °C for 18 h under a nitrogen atmosphere. The mixture was poured into 300 mL of stirred methanol slowly, and the precipitated compound was collected by filtration and washed thoroughly by methanol and hot water. The crude product was filtered and recrystallized by DMF/methanol to afford 8.1 g (72% in yield) of brown needles with an mp of 298–301 °C (by DSC at a scan rate of 2 °C min<sup>-1</sup>). FTIR (KBr): 1309, 1580 cm<sup>-1</sup> (—NO<sub>2</sub> stretch).

<sup>1</sup>H NMR (500 MHz, DMSO-*d*<sub>6</sub>,  $\delta$ , ppm): 3.89 (s, 6H, —OCH<sub>3</sub>), 7.07 (dd,  $J$  = 8.9, 2.0 Hz, 2H, H<sub>b</sub>), 7.35 (d,  $J$  = 9.1 Hz, 4H, H<sub>f</sub>), 7.42 (d,  $J$  = 8.9 Hz, 2H, H<sub>c</sub>), 7.50 (d,  $J$  = 8.5 Hz, 2H, H<sub>e</sub>), 7.71 (d,  $J$  = 8.5 Hz, 2H, H<sub>d</sub>), 7.83 (d,  $J$  = 2.0 Hz, 2H, H<sub>a</sub>), 8.24 (d,  $J$  = 9.1 Hz, 4H, H<sub>g</sub>). <sup>13</sup>C NMR (125 MHz, DMSO-*d*<sub>6</sub>,  $\delta$ , ppm): 55.62 (—OCH<sub>3</sub>), 103.28 (C<sup>2</sup>), 110.85 (C<sup>5</sup>), 115.26 (C<sup>4</sup>), 122.70 (C<sup>12</sup>), 123.40 (C<sup>1</sup>), 125.58 (C<sup>13</sup>), 127.50 (C<sup>8</sup>), 128.60 (C<sup>9</sup>), 132.29 (C<sup>7</sup>), 134.99 (C<sup>6</sup>), 138.02 (C<sup>10</sup>), 142.19 (C<sup>14</sup>), 151.49 (C<sup>11</sup>), 153.84 (C<sup>3</sup>).

**4,4'-Diamino-4''-(3,6-dimethoxycarbazol-9-yl)triphenylamine (6)**

In a 1-L three-neck round-bottomed flask equipped with a stirring bar and a nitrogen inlet, 2.8 g (0.005 mol) of dinitro compound **5** and 0.1 g of 10% Pd/C were dissolved/suspended in 500 mL of ethanol. The suspension solution was heated to reflux under a nitrogen atmosphere, and 3 mL of hydrazine monohydrate was added slowly to the mixture, then the solution was stirred at reflux temperature. After a further 16 h of reflux, the solution was filtered to remove Pd/C, and the filtrate was cooled under a nitrogen atmosphere to grow colorless crystals. The products were collected by filtration and dried *in vacuo* at 80 °C; yield = 1.5 g (60%), mp = 228–330 °C (by DSC at 2 °C min<sup>-1</sup>). FTIR (KBr): 3360, 3455 cm<sup>-1</sup> (N—H stretch).

<sup>1</sup>H NMR (500 MHz, DMSO-*d*<sub>6</sub>,  $\delta$ , ppm) [for the peak assignments, see Fig. 1(a)]: 3.86 (s, 6H, —OCH<sub>3</sub>), 5.03 (s, 4H, —NH<sub>2</sub>), 6.59 (d,  $J$  = 8.6 Hz, 4H, H<sub>g</sub>), 6.76 (d,  $J$  = 8.9 Hz, 2H, H<sub>e</sub>), 6.95 (d,  $J$  = 8.6 Hz, 4H, H<sub>f</sub>), 7.00 (dd,  $J$  = 8.9, 2.0 Hz, 2H, H<sub>b</sub>), 7.20 (d,  $J$  = 8.8 Hz, 2H, H<sub>c</sub>), 7.21 (d,  $J$  = 8.9 Hz, 2H,

H<sub>d</sub>), 7.76 (d,  $J$  = 2.0 Hz, 2H, H<sub>a</sub>). <sup>13</sup>C NMR (125 MHz, DMSO-*d*<sub>6</sub>,  $\delta$ , ppm) [for the peak assignments, see Fig. 1(b)]: 55.60 (—OCH<sub>3</sub>), 103.11 (C<sup>2</sup>), 110.37 (C<sup>8</sup>), 114.81 (C<sup>13</sup>), 115.03 (C<sup>4</sup>), 116.38 (C<sup>9</sup>), 122.61 (C<sup>1</sup>), 126.62 (C<sup>7</sup>), 126.76 (C<sup>5</sup>), 127.70 (C<sup>12</sup>), 135.33 (C<sup>11</sup>), 135.91 (C<sup>6</sup>), 145.98 (C<sup>14</sup>), 148.69 (C<sup>10</sup>), 153.28 (C<sup>3</sup>).

**Polymer Synthesis**

The synthesis of polyamide **8b** is used as an example to illustrate the general synthetic route. A mixture of 0.3504 g (0.7 mmol) of the diamine monomer **6**, 0.1105 g (0.7 mmol) of 4,4'-dicarboxydiphenyl ether (**7b**), 0.15 g of calcium chloride, 0.7 mL of triphenyl phosphite (TPP), 0.2 mL of pyridine, and 1.5 mL of NMP was heated with stirring at 120 °C for 3 h. The obtained highly viscous polymer solution was poured slowly into 150 mL of stirring methanol giving rise to a stringy, fiber-like precipitate that was collected by filtration, washed thoroughly with hot water and methanol, and dried under vacuum at 100 °C. Reprecipitations from DMAc into methanol were carried out twice for further purification. The inherent viscosity of the obtained polyamide **8b** was 0.52 dL g<sup>-1</sup>, measured at a concentration of 0.5 g dL<sup>-1</sup> in DMAc-5 wt % LiCl at 30 °C. The IR spectrum of **8b** (film) exhibited characteristic amide absorption bands at 3300 cm<sup>-1</sup> (N—H stretch) and 1655 cm<sup>-1</sup> (amide carbonyl stretch).

<sup>1</sup>H NMR (500 MHz, DMSO-*d*<sub>6</sub>,  $\delta$ , ppm) [for the peak assignments, see Fig. 2]: 3.87 (s, 6H, —OCH<sub>3</sub>), 7.03 (d,  $J$  = 8.9 Hz, 2H, H<sub>e</sub>), 7.20 (three overlapped doublets, 10H, H<sub>b</sub> + H<sub>f</sub> + H<sub>i</sub>), 7.31 (d,  $J$  = 8.9 Hz, 2H, H<sub>d</sub>), 7.44 (d,  $J$  = 8.8 Hz, 2H, H<sub>c</sub>), 7.79 (s, 6H, H<sub>a</sub> + H<sub>g</sub>), 8.05 (d,  $J$  = 8.6 Hz, 4H, H<sub>h</sub>), 10.27 (s, 2H, amide).

**Preparation of the Polyamide Films**

A solution of polymer was made by dissolving about 0.5 g of the polyamide sample in 10 mL of hot DMAc. The homogeneous solution was poured into a 9-cm glass Petri dish, which was placed in a 90 °C oven for 5 h to remove most of the solvent; then the semidried film was further dried *in vacuo* at 150 °C for 8 h. The obtained films were about 30–50  $\mu$ m in thickness and were used for X-ray diffraction measurements, solubility tests, and thermal analyses.

**Measurements**

Infrared spectra were recorded on a Horiba FT-720 FTIR spectrometer. Elemental analyses were run in a Heraeus VarioEL-III CHNS elemental analyzer. <sup>1</sup>H and <sup>13</sup>C NMR spectra were measured on a Bruker AVANCE-500 FT-NMR spectrometer using tetramethylsilane as the internal standard. The inherent viscosities were determined at 0.5 g dL<sup>-1</sup> concentration using Cannon-Fenske viscometer at 30 °C. Weight-average molecular weight ( $M_w$ ) and number-average molecular weight ( $M_n$ ) were obtained *via* gel permeation chromatography (GPC) on the basis of polystyrene calibration using Waters 2410 as an apparatus and NMP as the eluent. Wide-angle X-ray diffraction (WAXD) measurements were performed at room temperature (ca. 25 °C) on a Shimadzu XRD-6000 X-ray diffractometer (40 kV, 20 mA), using graphite-monochromatized Cu-K $\alpha$  radiation. Thermogravimetric analysis (TGA) was conducted with a

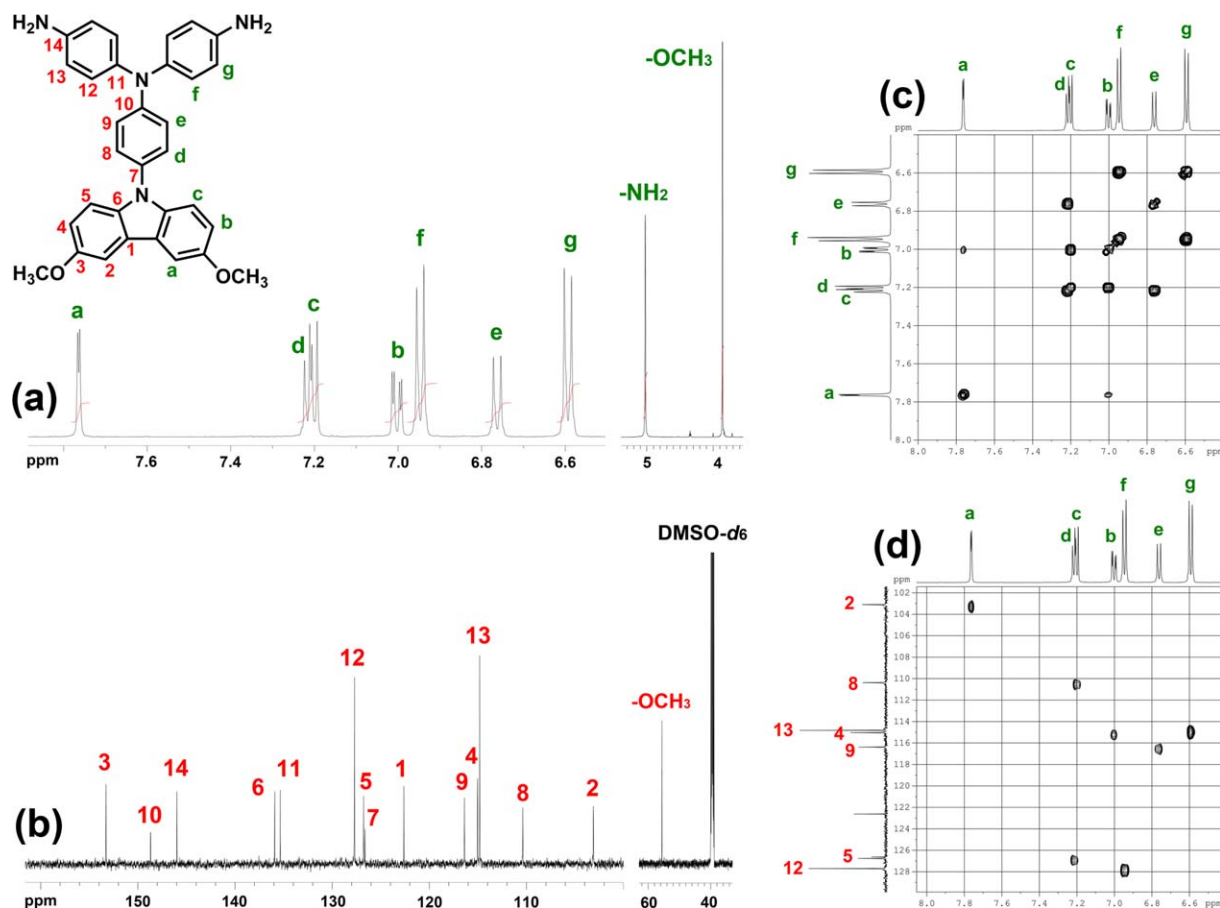


**FIGURE 1** (a)  $^1\text{H}$  NMR, (b)  $^{13}\text{C}$  NMR, (c) H-H COSY, and (d) C-H HMQC spectra of diamine monomer **6** in DMSO- $d_6$ . [Color figure can be viewed in the online issue, which is available at [wileyonlinelibrary.com](http://wileyonlinelibrary.com).]

PerkinElmer Pyris 1 TGA. Experiments were carried out on approximately 3–5 mg film samples heated in flowing nitrogen or air (flow rate =  $20\text{ cm}^3\text{ min}^{-1}$ ) at a heating rate of  $20\text{ }^\circ\text{C min}^{-1}$ . DSC analyses of the polyamides were performed on a PerkinElmer Pyris 1 DSC at a scan rate of  $20\text{ }^\circ\text{C min}^{-1}$  under a nitrogen flow ( $20\text{ cm}^3\text{ min}^{-1}$ ). Thermomechanical analysis (TMA) of the polymer film was conducted with a PerkinElmer TMA 7 instrument. The TMA experiments were conducted from  $50$  to  $350\text{ }^\circ\text{C}$  at a scan rate of  $10\text{ }^\circ\text{C min}^{-1}$  with a penetration probe  $1.0\text{ mm}$  in diameter under an applied constant load of  $10\text{ mN}$ . Softening temperatures ( $T_s$ ) were taken as the onset temperatures of probe displacement on the TMA traces. Absorption spectra were measured with an Agilent 8453 UV-visible diode array spectrophotometer. Electrochemistry was performed with a CH Instruments 611c electrochemical analyzer. Cyclic voltammetry (CV) was conducted with the use of a three-electrode cell in which ITO (polymer films area about  $1\text{ cm}^2$ ,  $0.8 \times 1.25\text{ cm}^2$ ) was used as a working electrode. A platinum wire was used as an auxiliary electrode. All cell potentials were taken with the use of an ALS RE-1B (Ag/AgCl,  $3\text{M NaCl}$ ) reference electrode. Ferrocene was used as an external reference for calibration ( $+0.44\text{ V}$  vs. Ag/AgCl). Voltammograms are presented with the positive/negative potential pointing to the right/left with increasing anodic/decreasing cathodic current pointing upward/downward. Spec-

troelectrochemistry analyses were carried out with an electrolytic cell, which was composed of a  $1\text{ cm}$  cuvette, ITO as a working electrode, a platinum wire as an auxiliary electrode, and a Ag/AgCl reference electrode. Absorption spectra in the spectroelectrochemical experiments were also measured with an Agilent 8453 UV-visible diode array spectrophotometer.

## RESULTS AND DISCUSSION

### Monomer Synthesis

The new aromatic diamine monomer, 4,4'-diamino-4''-(3,6-dimethoxycarbazol-9-yl)triphenylamine (**6**), was synthesized starting from carbazole by a reaction sequence as shown in Scheme 1. 3,6-Dibromocarbazole (**1**) was synthesized by bromination of carbazole with NBS. Direct methoxide displacement of bromine from compound **1** by using MeONa and CuI in DMF gave 3,6-dimethoxycarbazole (**2**). The intermediate compound, 3,6-dimethoxy-9-(4-nitrophenyl)carbazole (**3**), was synthesized by nucleophilic aromatic fluoro-displacement reaction of *p*-fluoronitrobenzene with compound **2** in the presence of CsF. Reduction of the nitro group of compound **3** by means of hydrazine and Pd/C gave 3,6-dimethoxy-9-(4-aminophenyl)carbazole (**4**). The target diamine monomer **6** was prepared by hydrazine Pd/C-catalyzed reduction of 4,4'-dinitro-4''-(3,6-dimethoxy-carbazol-9-yl)triphenylamine (**5**) resulting from the



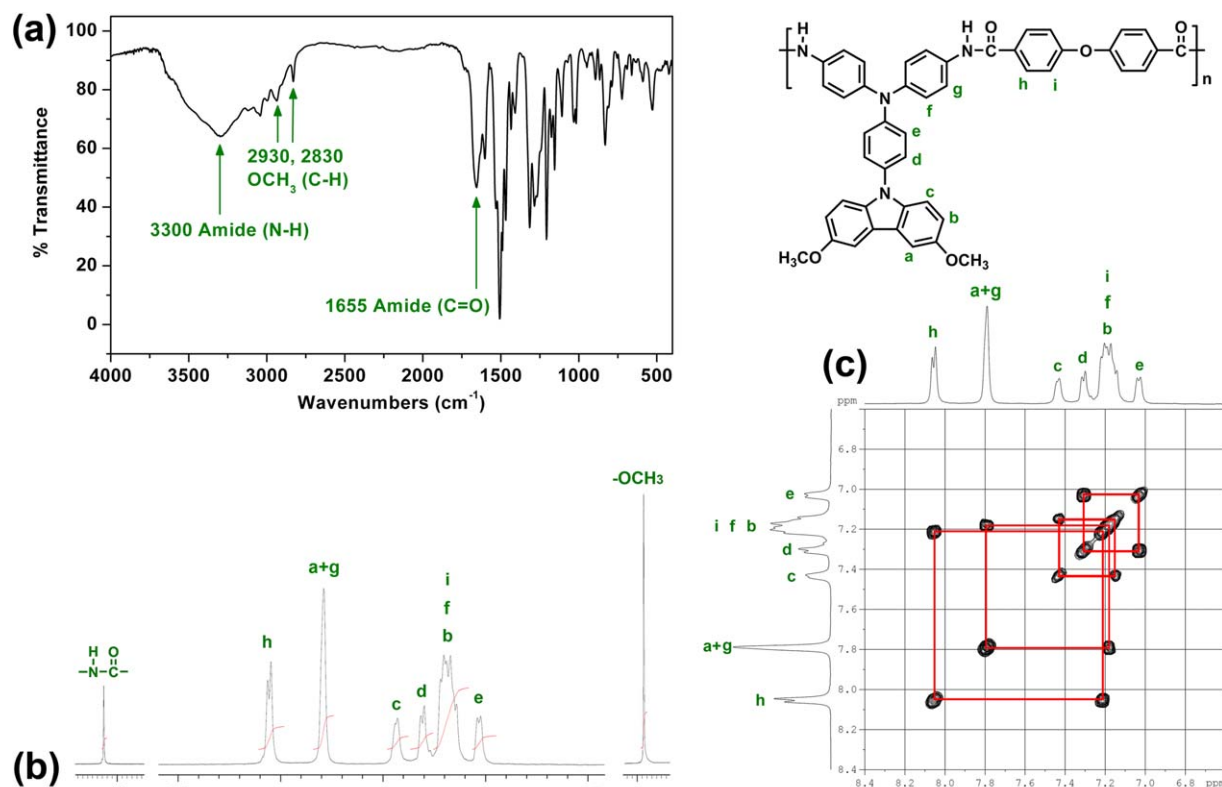
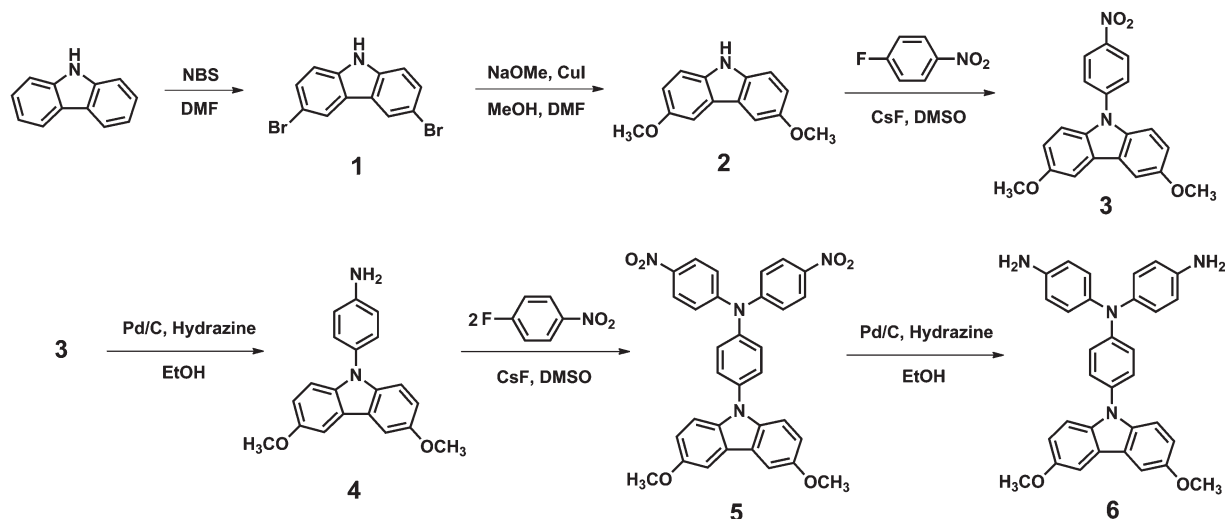


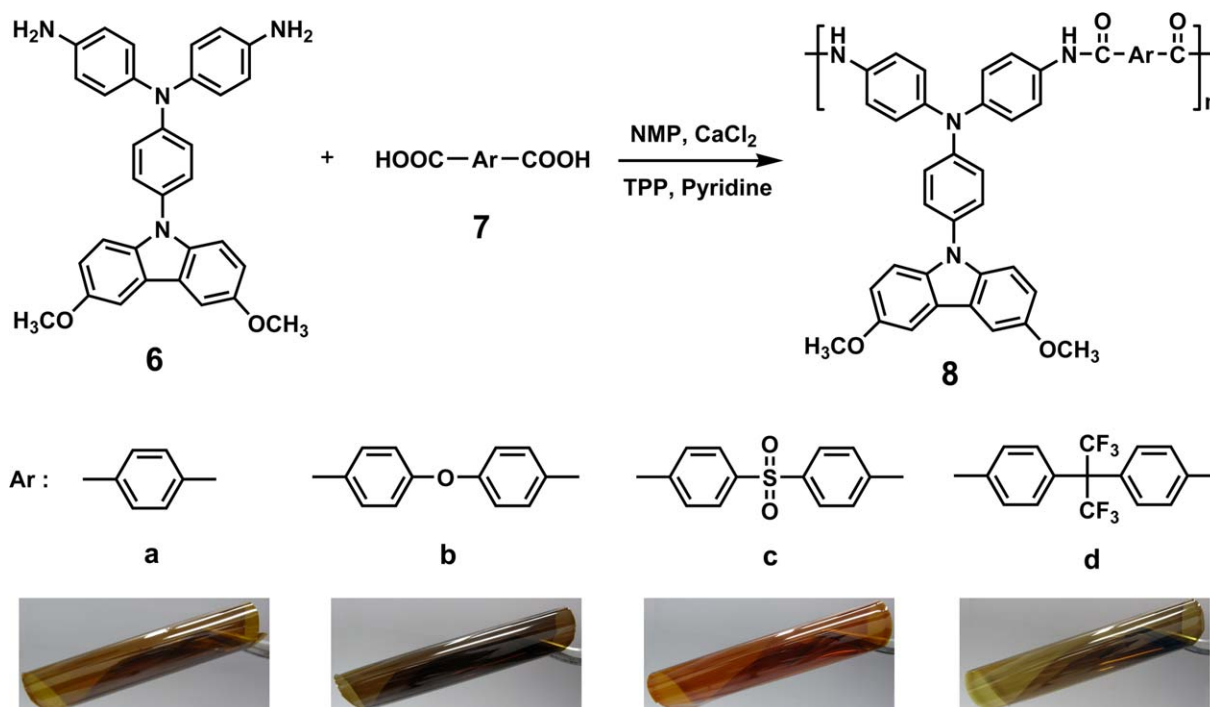
**FIGURE 2** (a) IR, (b)  $^1\text{H}$  NMR, and (c) aromatic portion of the H-H COSY spectrum of polyamide **8b** in  $\text{DMSO}-d_6$ . [Color figure can be viewed in the online issue, which is available at [wileyonlinelibrary.com](http://wileyonlinelibrary.com).]

$\text{CsF}$ -assisted  $N,N$ -diarylation reaction of compound **4** with two equivalent amount of  $p$ -fluoronitrobenzene. The structures of all the synthesized compounds were confirmed by IR and NMR analyses. The FTIR spectra of compounds **1–6** are shown in Supporting Information Figure S1. The IR spectrum of compound **1** shows the secondary  $\text{N-H}$  stretching absorption at  $3423\text{ cm}^{-1}$ . After methoxylation, the IR spectrum of dimethoxy compound **2** gave rise to a symmetric  $-\text{CH}_3$  stretching absorption at about  $2830\text{ cm}^{-1}$  and an asymmetric  $-\text{CH}_3$

stretching absorption at about  $2940\text{ cm}^{-1}$ . The nitro groups of compounds **3** and **5** gave two characteristic bands at around  $1580\text{--}1590$  and  $1300\text{--}1330\text{ cm}^{-1}$ , respectively ( $-\text{NO}_2$  asymmetric and symmetric stretching). After reduction to **4** and **6**, the characteristic absorptions of the nitro group disappeared and the primary amino group showed the typical absorption pair in the range  $3400\text{--}3200\text{ cm}^{-1}$  due to  $\text{N-H}$  stretching. The  $^1\text{H}$  and  $^{13}\text{C}$  NMR spectra of the intermediate compounds **1** to **5** are also shown in Supporting Information



**SCHEME 1** Synthetic pathway of the target diamine monomer **6**.



**SCHEME 2** Synthesis of aromatic polyamides **8a–8d**. Photographs show the appearances of their solution-cast films. [Color figure can be viewed in the online issue, which is available at [wileyonlinelibrary.com](http://wileyonlinelibrary.com).]

Figures S2–S6.  $^1\text{H}$  NMR,  $^{13}\text{C}$  NMR, and two-dimensional (2D) NMR spectra of the target diamine monomer **6** are compiled in Figure 1. The  $^1\text{H}$  NMR spectra confirm that the nitro groups have been completely transformed into amino groups by the high field shift of the aromatic protons and the resonance signals at around 5.0 ppm corresponding to the amino protons. Assignments of each carbon and proton assisted by the 2D NMR spectra are also indicated in these spectra, and they agree well with the proposed molecular structure of **6**.

### Polymer Synthesis

According to the phosphorylation technique first described by Yamazaki et al.,<sup>22</sup> a series of novel aromatic polyamides **8a–8d** with (3,6-dimethoxycarbazol-9-yl)-substituted TPA units were synthesized from the diamine monomer **6** with various aromatic dicarboxylic acids **7a–7d** using TPP and

pyridine as condensing agents (Scheme 2). All the polymerizations proceeded homogeneously throughout the reaction and afforded clear and highly viscous polymer solutions, and the products precipitated in a tough, fiber-like form when the resulting polymer solutions were slowly poured into stirring methanol. As shown in Table 1, the obtained polyamides had inherent viscosities in the range of 0.52–0.57 dL g<sup>−1</sup>. All the polyamides could be solution-cast into flexible and tough films (see the photos shown in Scheme 2), indicating high molecular weight polymers. The GPC measurement of these polyamides showed weight-average molecular weights ( $M_w$ ) in the range of 43,000–57,000 and polydispersity index ( $M_w/M_n$ ) of 2.46–2.49. The formation of polyamides was also confirmed by IR and NMR spectroscopy. Typical IR and NMR spectra for polyamide **8b** are given in Figure 2. The characteristic IR absorption bands of the amide group appeared

**TABLE 1** Inherent Viscosity, Molecular Weights and Solubility Behavior of Polyamides

Polymer Code	$\eta_{\text{inh}}^a$ (dL g <sup>−1</sup> )	GPC Data <sup>b</sup>			Solubility <sup>d</sup> in Various Solvents <sup>e</sup>					
		$M_n$	$M_w$	PDI <sup>c</sup>	NMP	DMAc	DMF	DMSO	<i>m</i> -Cresol	THF
<b>8a</b>	0.57	17,500	43,000	2.46	++	++	++	++	+h	+-
<b>8b</b>	0.52	17,500	43,500	2.49	++	++	++	++	+-	+-
<b>8c</b>	0.54	23,000	57,000	2.48	++	++	++	++	+h	+-
<b>8d</b>	0.56	20,500	50,500	2.46	++	++	++	++	+h	++

<sup>a</sup> Inherent viscosity measured at a concentration of 0.5 dL g<sup>−1</sup> in DMAc – 5 wt % LiCl at 30 °C.

<sup>b</sup> Calibrated with polystyrene standards, using NMP as the eluent at a constant flow rate of 0.5 mL min<sup>−1</sup> at 40 °C.

<sup>c</sup> Polydispersity Index ( $M_w/M_n$ ).

<sup>d</sup> Solubility: ++: soluble at room temperature; +-: partially soluble; +h: soluble on heating.

<sup>e</sup> Solvent: NMP, *N*-methyl-2-pyrrolidone; DMAc, *N,N*-dimethylacetamide; DMF, *N,N*-dimethylformamide; DMSO, dimethyl sulfoxide; THF, tetrahydrofuran.

**TABLE 2** Thermal Properties of Polyamides

Polymer <sup>a</sup> Code	$T_g^b$ (°C)	$T_s^c$ (°C)	$T_d^d$ at 10 wt % Loss (°C)		Char Yield <sup>e</sup> (%)
			In N <sub>2</sub>	In Air	
<b>8a</b>	296	295	507	496	70
<b>8b</b>	277	277	512	504	72
<b>8c</b>	308	306	492	480	66
<b>8d</b>	296	295	508	507	72

<sup>a</sup> The polymer film samples were heated at 300 °C for 1 h prior to all the thermal analyses.

<sup>b</sup> The samples were heated from 50 to 400 °C at a scan rate of 20 °C min<sup>-1</sup> followed by rapid cooling to 50 °C at -200 °C min<sup>-1</sup> in nitrogen. The midpoint temperature of baseline shift on the subsequent DSC trace (from 50 to 400 °C at heating rate 20 °C min<sup>-1</sup>) was defined as  $T_g$ .

<sup>c</sup> Softening temperature measured by TMA using a penetration method.

<sup>d</sup> Decomposition temperature at which a 10% weight loss was recorded by TGA at a heating rate of 20 °C min<sup>-1</sup>.

<sup>e</sup> Residual weight percentages at 800 °C under nitrogen flow.

around 3300 (N—H stretching) and 1655 cm<sup>-1</sup> (amide carbonyl). With the help of 2D NMR spectroscopy, all the peaks could be readily assigned to the hydrogen atoms in the repeating unit. The resonance peak appearing at 10.27 ppm in the <sup>1</sup>H NMR spectrum also supports the formation of amide linkages.

### Polymer Properties

#### Basic Characterization

The solubility behavior of polyamides was tested qualitatively, and the results are also listed in Table 1. All the polyamides were readily soluble in dipolar organic solvents such as NMP, DMAc, DMF, and DMSO. Polyamide **8d** also showed good solu-

bility in less polar solvents like THF because of the additional contribution of the hexafluoroisopropylidene [ $-C(CF_3)_2-$ ] fragment in the polymer backbone. The high solubility of these polyamides can be attributed in part to the introduction of bulky, packing-disruptive 3,6-dimethoxy-CzTPA units in the polymer structure. Thus, the excellent solubility makes these polymers potential candidates for practical applications by simple spin- or dip-coating processes to afford high performance thin films for optoelectronic devices. As it was mentioned earlier, all the polyamides could be solution-cast into transparent, flexible, and strong films. The WAXD studies of these film samples indicated that all the polymers were essentially amorphous (Supporting Information Fig. S7).

**TABLE 3** Redox Potentials and Energy Levels of Polyamides

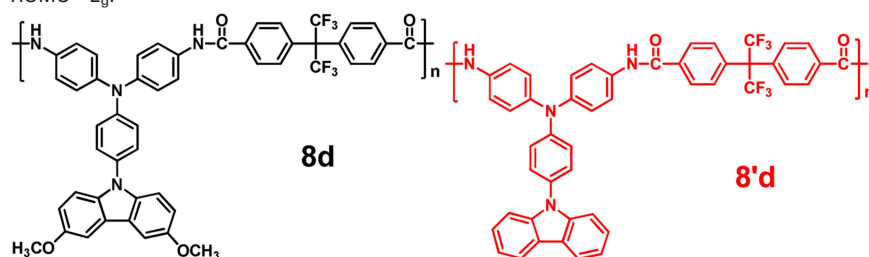
Polymer Code	Absorption <sup>a</sup>		Oxidation <sup>b</sup> (V)			$E_g^c$ (eV)	HOMO <sup>d</sup> (eV)	LUMO <sup>d</sup> (eV)
	$\lambda_{max}$ (nm)	$\lambda_{onset}$ (nm)	$E_{onset}$	$E_{1/2}^{OX1}$	$E_{1/2}^{OX2}$			
<b>8a</b>	312	429	0.64	0.76	1.04	2.89	5.08	2.20
<b>8b</b>	312	400	0.65	0.76	1.04	3.10	5.09	1.99
<b>8c</b>	313	466	0.65	0.77	1.05	2.72	5.09	2.37
<b>8d</b>	312	406	0.66	0.78	1.06	3.05	5.10	2.05
<b>8'd</b>	343	400	0.75	0.90	1.27	3.10	5.19	2.09

<sup>a</sup> Measured as thin films.

<sup>b</sup> From cyclic voltammograms versus Ag/AgCl in CH<sub>3</sub>CN.  $E_{1/2}$ : Average potential of the redox couple peaks.

<sup>c</sup> The data were calculated from polymer films by the equation:  $E_g = 1240/\lambda_{onset}$  (energy gap between HOMO and LUMO).

<sup>d</sup> The HOMO energy levels were calculated from cyclic voltammetry and were referenced to ferrocene (4.8 eV; onset = 0.36 V); LUMO = HOMO -  $E_g$ .



### Thermal Properties

The thermal properties of all the polyamides were investigated by TGA, DSC, and TMA techniques. The pertinent data are summarized in Table 2. Typical TGA curves of a representative polyamide **8d** in both air and nitrogen atmospheres are illustrated in Supporting Information Figure S8. All the polymers exhibited good thermal stability with insignificant weight loss up to 480 °C in both air and nitrogen atmospheres. The decomposition temperatures ( $T_d$ ) at a 10% weight-loss of the polyamides in nitrogen and air were recorded in the range of 492–512 and 480–507 °C, respectively. The amount of carbonized residue (char yield) of these polymers in nitrogen atmosphere was more than 66% at 800 °C. The high char yields of these polymers can be ascribed to their high aromatic content. The glass-transition temperatures ( $T_g$ ) of these polyamides were observed in the range of 277–308 °C by DSC. Polyamide **8b** showed the lowest  $T_g$  (277 °C) among this series polyamides because of the presence of flexible ether linkage in its diacid component. The softening temperatures ( $T_s$ ) of the polymer films were determined from the onset temperature of the probe displacement on the TMA trace. In most cases, the  $T_s$  values of the polyamides obtained by TMA are comparable to the  $T_g$  values measured by the DSC experiments. Overall, the thermal analysis results reveal that these polyamides exhibit good thermal stability.

### Electrochemical Properties

The electrochemical behavior of the polyamides was investigated by CV conducted for the cast film on an ITO-coated glass substrate as working electrode in dry acetonitrile ( $\text{CH}_3\text{CN}$ ) containing 0.1 M of tetrabutylammonium perchlorate ( $\text{Bu}_4\text{NClO}_4$ ) as an electrolyte under nitrogen atmosphere. The derived oxidation potentials are summarized in Table 3. The representative cyclic voltammograms of polyamides **8d** (with methoxy substituents on the active sites of the carbazole unit) and **8'd** (without methoxy groups on the carbazole unit) are illustrated in Figure 3 for comparison. Polyamide **8d** exhibits two reversible oxidation redox couples with half-wave potentials ( $E_{1/2}$ ) of 0.76 and 1.03 V during the oxidative scan, corresponding to successive one electron removal from the TPA and carbazole moieties. Polyamide **8d** exhibited excellent redox reversibility when repeatedly scanning between 0.0 and 1.3 V at a scan rate of 50  $\text{mV s}^{-1}$ . The high electrochemical stability of polyamide **8d** can be attributable to the fact that the active sites (the C-3 and C-6 positions) of the carbazole are blocked with methoxy groups. The referenced polyamide **8'd** shows higher oxidation potentials as compared to polyamide **8d**, with  $E_{1/2}$  values of 0.90 and 1.27 V in the first CV scan. Without blocking the electrochemically active sites of the carbazole, the oxidation process of **8'd** is not reversible. As shown in Figure 3(b), two oxidation peaks were observed at about 1.02 and 1.52 V in the first positive potential scan of **8'd**. From the first reverse negative potential scan, we detected three cathodic peaks at 1.28, 1.01, and 0.77 V. In the second scan, two new oxidation peaks appeared at about 1.25 and 1.42 V, which was the complementary anodic process of the

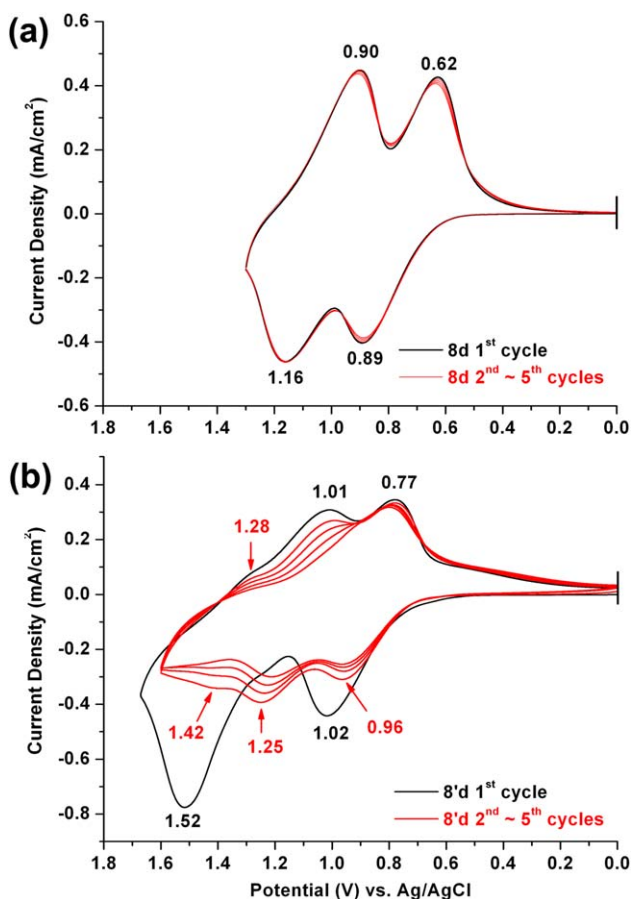
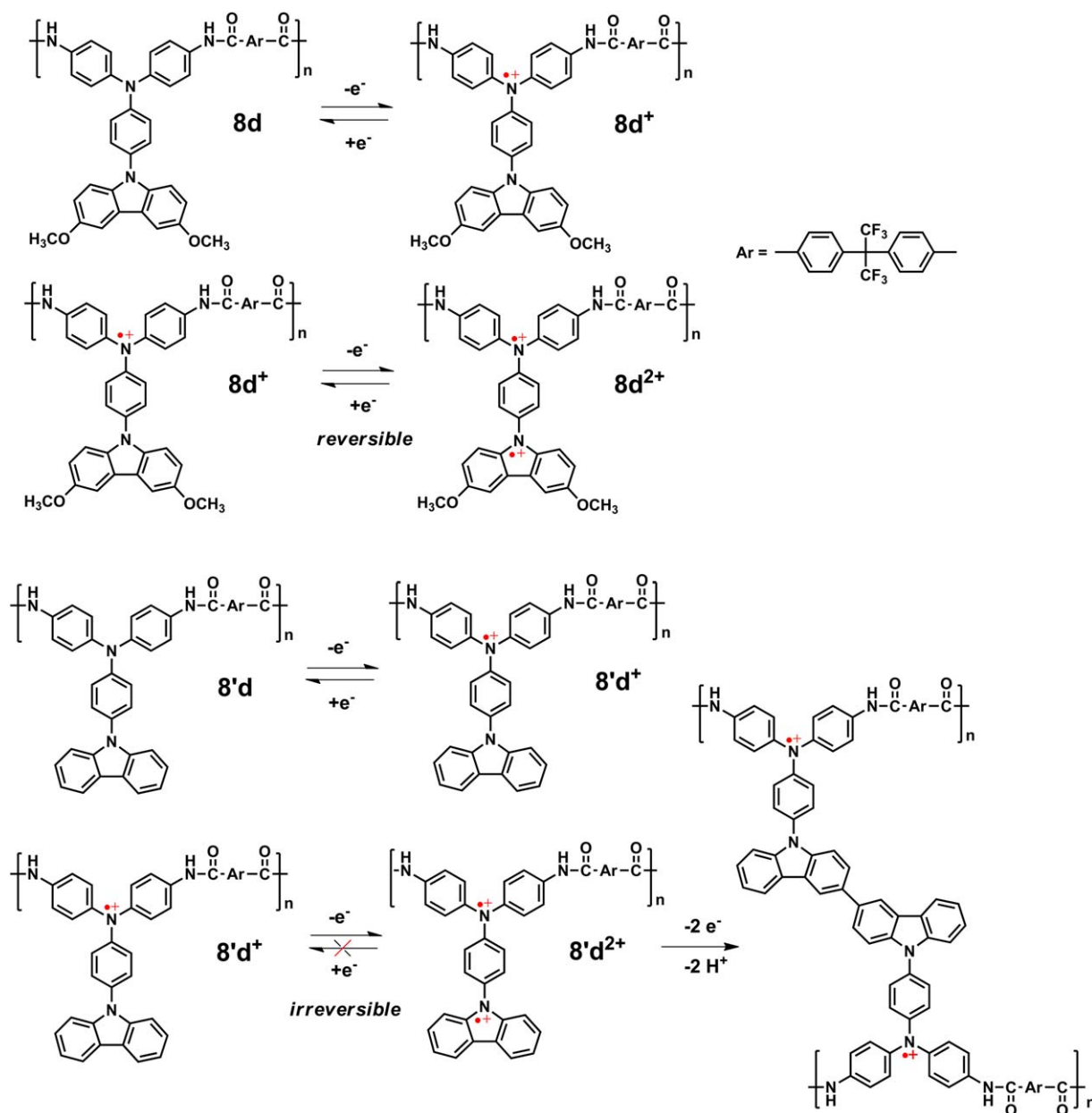


**FIGURE 3** Repeated CV diagrams of the cast films of polyamides (a) **8d** and (b) **8'd** on the ITO-coated glass substrate in 0.1 M  $\text{Bu}_4\text{NClO}_4/\text{CH}_3\text{CN}$  at a scan rate of 50  $\text{mV s}^{-1}$ . [Color figure can be viewed in the online issue, which is available at [wileyonlinelibrary.com](http://wileyonlinelibrary.com).]

cathodic peak at 1.01 and 1.28 V. The observation of two new oxidation couples in the second scan indicates that the carbazole radical cations were involved in very fast electrochemical reactions that produced a new structure that was easier to oxidize than was the parent carbazole. As reported by Ambrose et al. in their pioneering works<sup>23</sup> devoted to anodic oxidation of carbazole and other *N*-substituted derivatives, ring-ring coupling is the predominant decay pathway. One possible coupling reaction of carbazolium radical cations to biscarbazole shown in Scheme 3 can be used to explain the irreversible oxidation process occurring in polyamide **8'd**. Thus, in the second CV curve of **8'd**, the second anodic peak corresponds to one-electron oxidation of the biscarbazole units to form radical cations, followed by oxidation to the dicationic species. Thus, the introduction of electron-donating methoxy group not only greatly prevents the coupling reaction but also slightly lowers the oxidation potentials of the present polyamides.

The HOMO (highest occupied molecular orbital) energy levels of the investigated polyamides were calculated from the oxidation onset potentials ( $E_{\text{onset}}$ ) and by comparison with





**SCHEME 3** The anodic oxidation pathways of polyamides **8d** and **8'd**. [Color figure can be viewed in the online issue, which is available at [wileyonlinelibrary.com](http://wileyonlinelibrary.com).]

ferrocene (4.8 eV; onset = 0.36 V). These data together with absorption spectra were then used to obtain the LUMO (lowest unoccupied molecular orbital) energy levels (Table 3). According to the HOMO and LUMO energy levels obtained, these polyamides appear to be appropriate as hole injection and transport materials.

### Spectroelectrochemistry

Following the electrochemical tests, the optical properties of the electrochromic films were evaluated by using spectroelectrochemistry at different applied potentials. The electrode preparations and solution conditions were identical to those used in CV. The polymers were drop-coated as films on ITO-

glass substrates and mounted in a spectroelectrochemical cell. Figure 4(a) presents the UV-vis-NIR absorption spectra of polyamide **8d** film at various applied potentials. In the neutral form, polyamide **8d** exhibited strong absorptions at 312 and 343 nm, characteristic for  $\pi-\pi^*$  transitions, but it was almost transparent in the visible and NIR regions. The band gap of polyamide **8d** was estimated to be 3.10 eV from the onset of the  $\pi-\pi^*$  transition at 400 nm. When the applied potential was gradually increased to 0.9 V, the absorption of  $\pi-\pi^*$  transition decreased while a new absorption peak at 424 nm grew up and a broad absorption centered at 771 nm in the visible region together with a broad band from 900 nm extending into the NIR region beyond

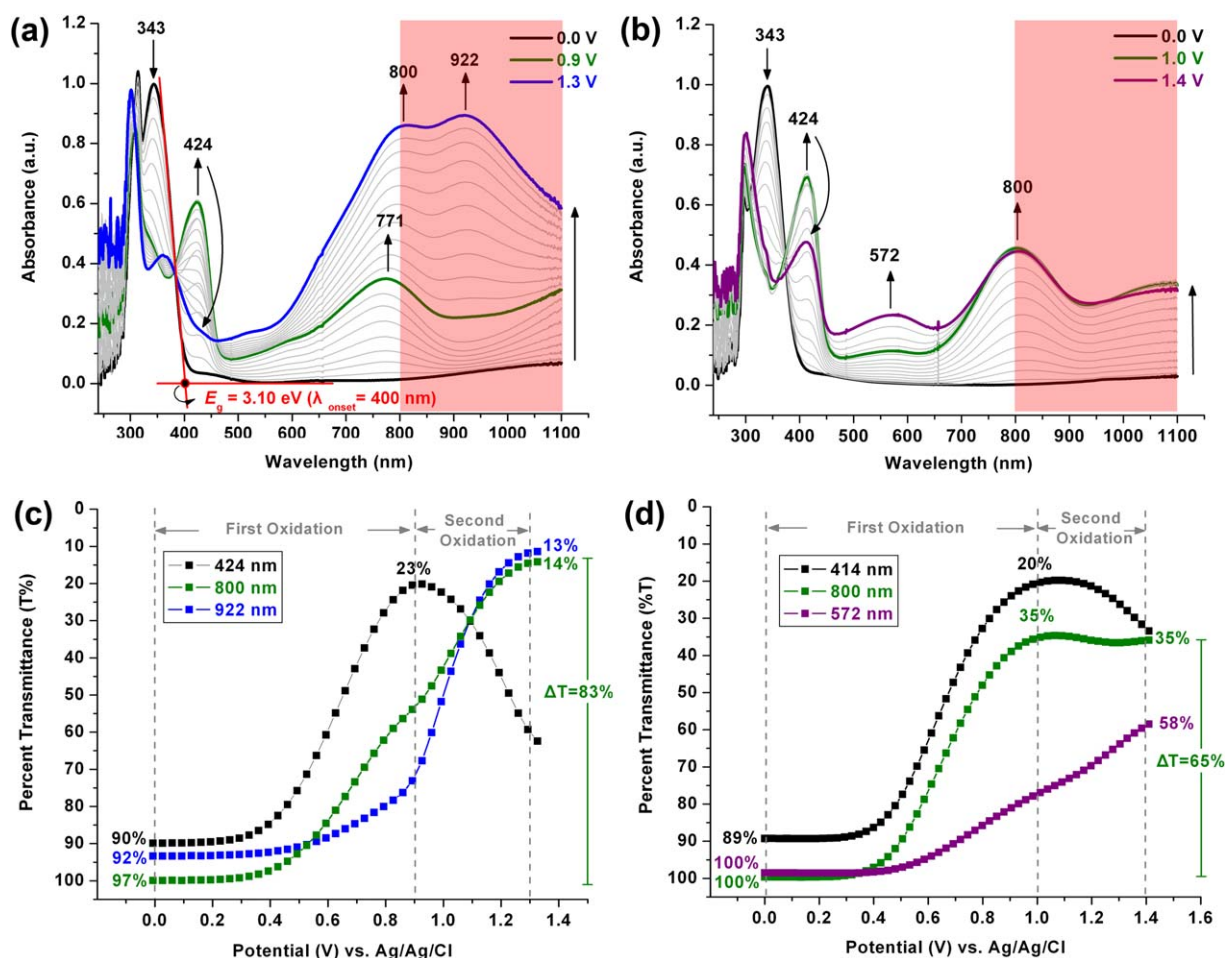


**FIGURE 4** Spectroelectrochemistry of the cast films of polyamides (a) **8d** and (b) **8'd** on the ITO-coated glass substrate in 0.1 M  $\text{Bu}_4\text{NClO}_4/\text{CH}_3\text{CN}$  at various applied potentials (vs. Ag/AgCl); Optical change in %T as a function of applied potential for the indicated absorption wavelengths for polyamides (c) **8d** and (d) **8'd**. [Color figure can be viewed in the online issue, which is available at [wileyonlinelibrary.com](http://www.wileyonlinelibrary.com).]

1100 nm gradually increased in intensity. As the potentials examined are similar to the first anodic process, the spectral changes are assigned to the radical cation (polaron) formation arising from the oxidation of TPA unit. The absorption band in the NIR region may be attributed to an intervalence charge transfer between states in which the positive charge is centered at different amino centers (TPA and carbazole).<sup>24</sup> Upon further oxidation at applied voltages to 1.3 V, the intensity of the absorption peak at 424 nm gradually decreased while the absorption peak at 800 nm gradually increased with a formation of a new strong absorption band centered at about 922 nm. The observed electronic absorption changes in the film of **8d** at various potentials are fully reversible and are associated with strong color changes; indeed, they even can be seen readily by the naked eye. The film of polyamide **8d** switches from a transmissive neutral state (nearly colorless) to a highly absorbing semioxidized state (yellowish green) and a fully oxidized state (blue). For comparison, the spectroelectrochemical series of polyamide **8'd** are shown in Figure 4(b). The

change of % transmittance for the absorption maxima of polyamides **8d** and **8'd** at various applied electrode potentials are depicted in Figure 4(c,d), respectively. It can be seen that polymer **8d** revealed a higher optical contrast (83%) in the NIR regions for blue coloring at the second oxidation stage than the referenced polymer **8'd** (65%) without the methoxy substituents on the carbazole unit at 800 nm when the applied potential was set at 1.3–1.4 V. This result may be explained by the irreversible second oxidation process associated with polyamide **8'd**. Therefore, the introduction of the methoxy group at the active sites of the carbazole unit not only enhances the redox stability but also improve the electrochromic contrast of these polymers.

As described earlier, the original structure of **8'd** might transform to a partially crosslinking structure via the oxidative coupling of the carbazoles (Scheme 3). In order to obtain a partially crosslinking film of polyamide **8'd**, the film of **8'd** on ITO-glass was repeatedly scanned between 0.0 and 1.5 V at  $50 \text{ mV s}^{-1}$  for 10 cycles. After that, the

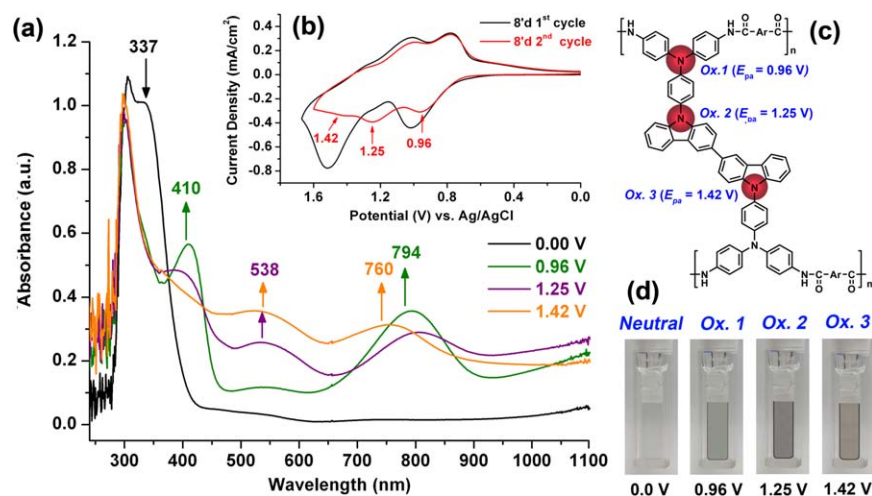


**FIGURE 5** (a) Spectral changes the crosslinking film of polyamide **8'd** on the ITO-coated glass substrate in 0.1 M  $\text{Bu}_4\text{NClO}_4/\text{CH}_3\text{CN}$  at various applied potentials. (b) The CV diagram for the first and second scans. (c) The possible electro-oxidation order for the amino centers in the repeating unit of crosslinked polyamide **8'd**. (d) The color changes of the polymer films at indicated applied electrode potentials. [Color figure can be viewed in the online issue, which is available at [wileyonlinelibrary.com](http://wileyonlinelibrary.com).]

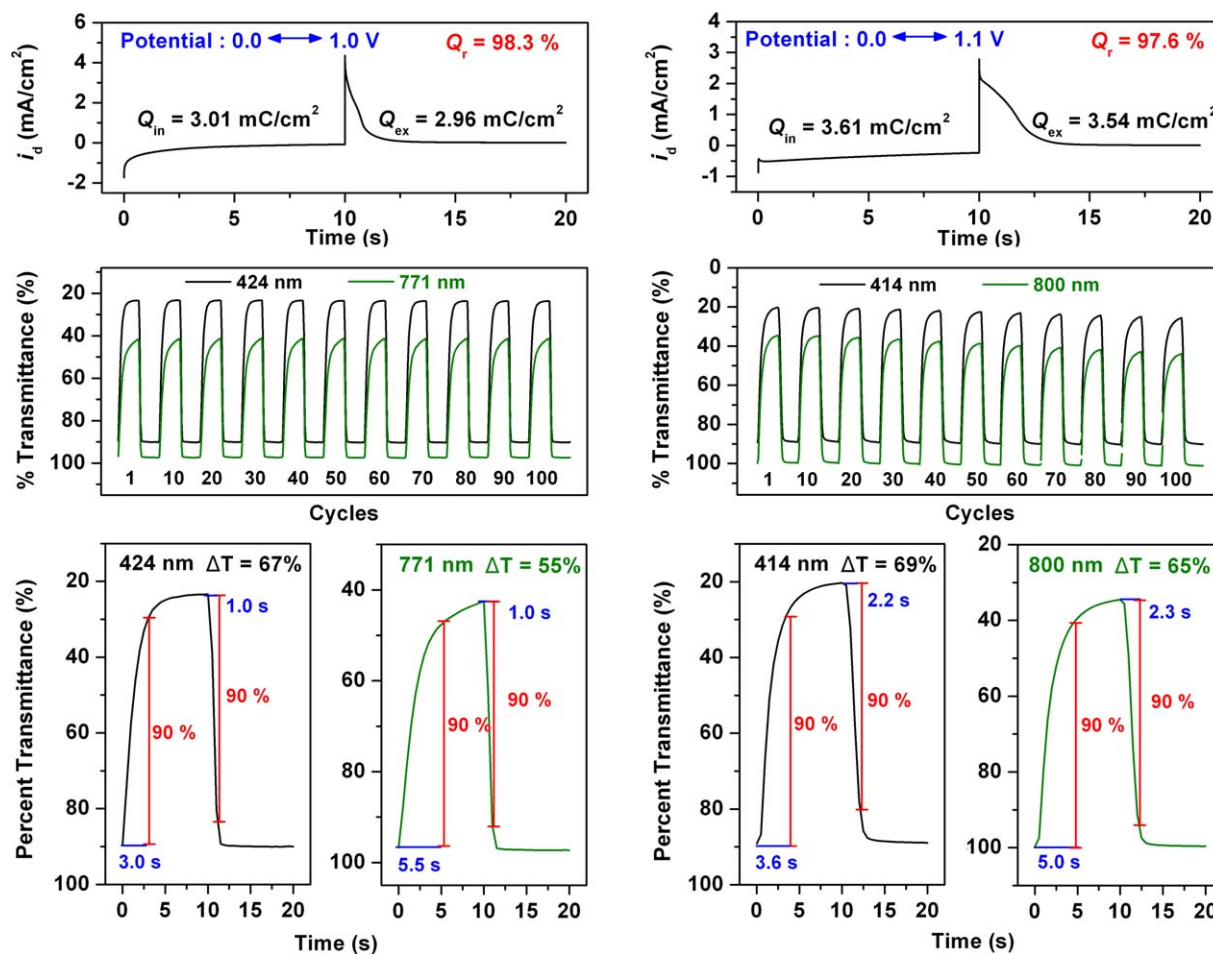


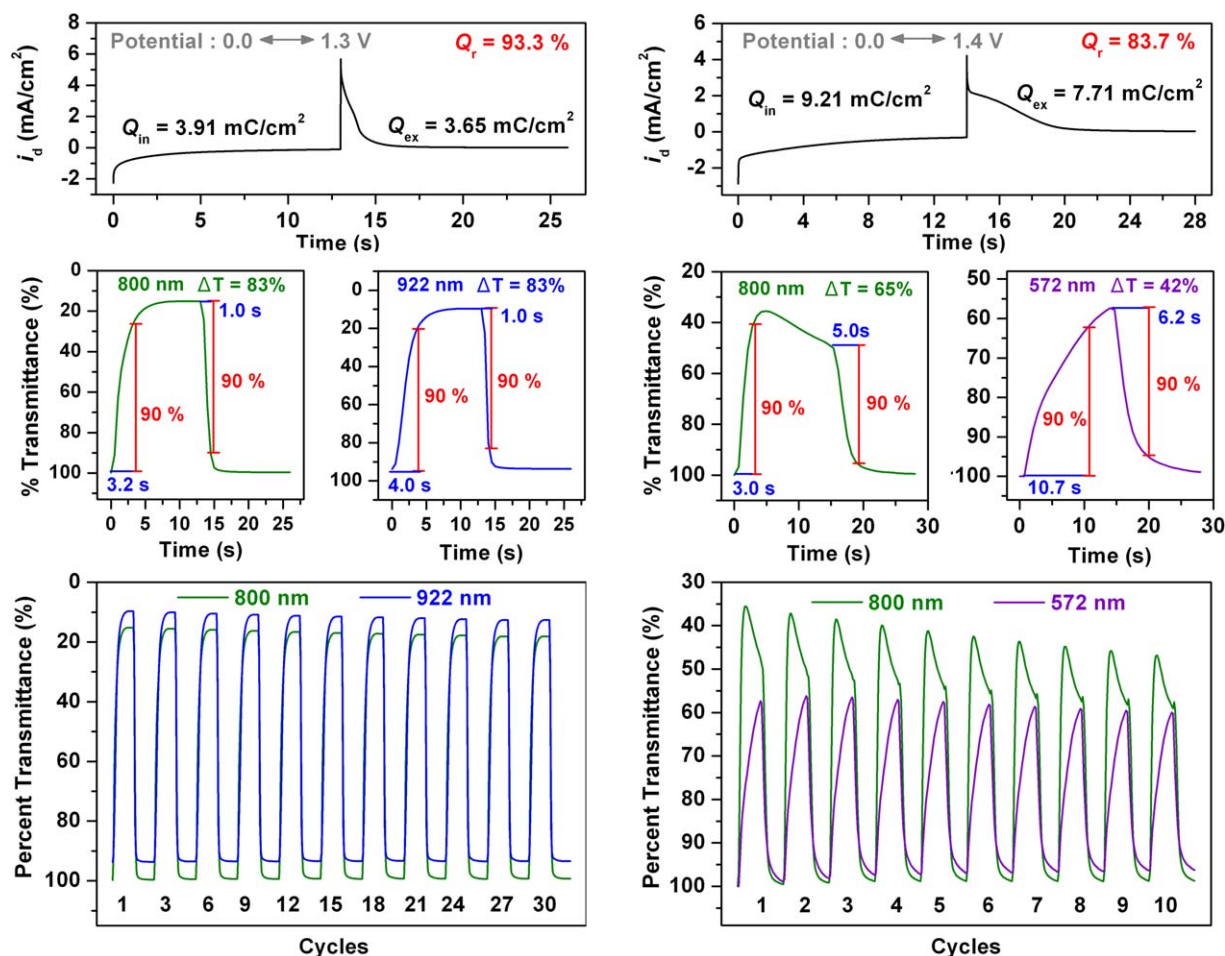
**FIGURE 6** Potential step absorbptometry of the cast films of polyamides **8'd** and **8'd** on the ITO-glass slide (coated area  $\sim 1 \text{ cm}^2$ ) (in  $\text{CH}_3\text{CN}$  with 0.1 M  $\text{Bu}_4\text{NClO}_4$  as the supporting electrolyte) by applying a potential step: (left) optical switching for polyamide **8'd** at potential 0.0 V ( 1.0 V and cycle time 10 s, monitored at  $\lambda_{\text{max}} = 424$  and 771 nm; (right) **8'd** at potential 0.0 V ( 1.1 V and cycle time 10 s, monitored at  $\lambda_{\text{max}} = 414$  and 800 nm. [Color figure can be viewed in the online issue, which is available at [wileyonlinelibrary.com](http://wileyonlinelibrary.com).]



spectroelectrochemical and electrochromic properties of the polymer film were investigated. After the first CV scan between 0.0 and 1.5 V, polyamide **8'd** displayed three peaks at around 0.96, 1.25, and 1.42 V in the subsequent CV scans [Fig. 5(b)]. The spectroelectrochemical behavior of the cross-linking polyamide **8'd** film is shown in Figure 5(a). When the applied potentials increased positively from 0 to 0.96, 1.25, and 1.42 V, respectively, corresponding to the first, second, and third electron oxidation, the characteristic absorption bands at 298 and 337 nm for neutral-form polyamide **8'd** decreased gradually and bathochromically shifted to 410 nm, accompanied by the concomitant formation of new broad long-wavelength absorption bands centered around 794, 538, and 760 nm, respectively. The film showed a multicolored electrochromism from colorless neutral state to pale green, purple, and orange oxidized states [Fig. 5(d)]. The possible oxidation order of the redox centers of polyamide **8'd** is proposed in Figure 5(c).

### Electrochromic Switching Studies





For the electrochromic switching studies, polymer films were cast on ITO-coated glass slides in the same manner as described above, and chronoamperometric and absorbance measurements were performed. While the films were switched, the absorbance at selected wavelengths was monitored as a function of time with UV-vis-NIR spectroscopy. Figure 6 depicts the optical transmittance at 424 and 771 nm as a function of time by applying square-wave potential steps between 0 and 1.0 V for a resident time of 10 s for polyamide **8d** and at 414 and 800 nm between 0 and 1.1 V for a resident time of 12 s for the referenced polyamide **8'd**. The response time was calculated at 90% of the full-transmittance change, because it is difficult to perceive any further color change with naked eye beyond this point. As shown in Figure 6, polyamide **8d** attained 90% of a complete coloring and bleaching in 3.0 and 1.0 s, respectively. The optical contrast measured as  $\Delta T\%$  of polyamide **8d** between



**FIGURE 7** Potential step absorptometry of the cast films of polyamides **8d** and **8'd** on the ITO-glass slide (coated area  $\sim 1 \text{ cm}^2$ ) (in  $\text{CH}_3\text{CN}$  with 0.1 M  $\text{Bu}_4\text{NClO}_4$  as the supporting electrolyte) by applying a potential step: (left) optical switching for polyamide **8d** at potential 0.0 V (1.3 V and cycle time 13 s, monitored at  $\lambda_{\text{max}} = 800$  and 922 nm; right) **8'd** at potential 0.0 V (1.4 V and cycle time 14 s, monitored at  $\lambda_{\text{max}} = 800$  and 572 nm. [Color figure can be viewed in the online issue, which is available at [www.interscience.wiley.com](http://www.interscience.wiley.com).]



**TABLE 4** Electrochromic Properties of Polyamides **8d** and **8'd**

Polymer	Doping Processes	$E$ (V)	Pulse Width (s)	$\lambda_{\max}^a$ (nm)	$\Delta T$ (%)	$t_{0.9}^c$ (s)	$t_{0.9}^b$ (s)	$\Delta OD^b$	$Q_d^c$ (mC cm $^{-2}$ )	$\eta^d$ (cm $^2$ C $^{-1}$ )	Neutral State	Oxidized State
<b>8d</b>	First p-doping	1.0	10	424	67	3.0	1.0	0.592	3.01	197		
				771	55	5.5	1.0	0.347		115		
	Second p-doping	1.3	13	800	83	3.2	1.0	0.841	3.91	215		
				922	79	4.0	1.0	0.850		217		
<b>8'd</b>	First p-doping	1.1	10	414	69	3.6	2.2	0.650	3.61	184		
				800	65	5.0	2.3	0.456		129		
	Second p-doping	1.4	14	800	65	3.0	5.0	0.456	9.21	50		
				572	42	10.7	6.2	0.237		26		

<sup>a</sup> Wavelength of absorption maximum.<sup>b</sup> Optical density ( $\Delta OD$ ) =  $\log[T_{\text{bleached}}/T_{\text{colored}}]$ , where  $T_{\text{bleached}}$  and  $T_{\text{colored}}$  are the maximum transmittance in the neutral and oxidized state, respectively.<sup>c</sup>  $Q_d$  is ejected charge, determined from the *in situ* experiments.<sup>d</sup> Coloration efficiency  $\eta = \Delta OD/Q_d$ .

neutral colorless and oxidized green states was found to be 67% at 424 nm. The referenced polyamide **8'd** attained 90% of a complete coloring and bleaching in 3.6 and 2.2 s, respectively. The optical contrast measured as  $\Delta T\%$  of polyamide **8'd** between neutral colorless and oxidized green states was found to be 69% at 800 nm. The amount of injected/ejected charge ( $Q_r$ ) were calculated by integration of the current density and time obtained from Figure 6 as 3.01 and 2.96 mC cm $^{-2}$  for oxidation and reduction processes of polyamide **8d** at the first oxidation stage, respectively. The ratio of the charge density was 98.3%, indicating that charge injected/ejected was highly reversible during the electrochemical reactions. While the switched potential was adjusted to the second oxidation stage from 0.0 to 1.3 V, the polyamide **8d** thin film required almost the same times for coloration and bleaching with 93.3% of

the ratio of the charge density (Fig. 7). The electrochromic CE ( $\eta = \Delta OD/Q$ ) and injected charge (electroactivity) after various switching steps were monitored and summarized in Table 4. After continuous 100 cyclic scanning at the first oxidation stage, the film of polyamide **8d** only showed 5.0% decay on coloration efficiency, which is much lower than that of corresponding **8'd** analog. As the applied switching potential increased to the second oxidation stage, the polyamide **8d** still showed little optical contrast loss during switching 30 cycles and a higher CE for the blue coloring (215 cm $^2$  C $^{-1}$  at 922 nm) (Table 5). However, the **8'd** film showed a moderate optical contrast loss at 800 nm after 10 full switches (Fig. 7). Therefore, the introduction of the methoxy group at the electrochemically active C-3 and C-6 sites of the carbazole unit enhances the redox and electrochromic stability of these polymers.

**TABLE 5** Optical and Electrochemical Data Collected for Coloration Efficiency Measurements of Polyamide **8d** and **8'd**

Cycle <sup>a</sup>	$\Delta T$ (%)		$\Delta OD^b$		$Q$ (mC cm $^{-2}$ ) <sup>c</sup>		$\eta$ (cm $^2$ C $^{-1}$ ) <sup>d</sup>		Decay(%) <sup>e</sup>	
	<b>8d</b>	<b>8'd</b>	<b>8d</b>	<b>8'd</b>	<b>8d</b>	<b>8'd</b>	<b>8d</b>	<b>8'd</b>	<b>8d</b>	<b>8'd</b>
1	67	69	0.592	0.650	3.01	3.61	197	184	0	0
10	67	68	0.592	0.642	3.02	3.61	196	178	0.5	3.3
20	67	68	0.590	0.640	3.01	3.60	196	177	0.5	3.8
30	66	67	0.586	0.631	3.00	3.59	195	176	1.0	4.3
40	66	66	0.582	0.621	2.99	3.58	194	174	1.5	5.4
50	65	65	0.580	0.609	2.99	3.58	194	170	1.5	7.6
60	65	65	0.576	0.597	2.99	3.56	193	167	2.0	9.2
70	64	64	0.570	0.583	2.98	3.54	191	164	3.0	10.9
80	64	64	0.562	0.575	2.97	3.53	189	163	4.0	11.4
90	64	64	0.558	0.565	2.97	3.53	188	160	4.6	12.5
100	63	63	0.555	0.553	2.96	3.50	187	158	5.0	13.6

<sup>a</sup> Switching between 0 and 1.0 V for **8d** and 0 and 1.1 V for **8'd** (vs. Ag/AgCl).<sup>b</sup> Optical density change at 424 nm for **8d** and 414 nm for **8'd**.<sup>c</sup> Ejected charge, determined from the *in situ* experiments.<sup>d</sup> Coloration efficiency is derived from the equation:  $\eta = \Delta OD/Q$ .<sup>e</sup> Decay of optical density change after cyclic scans.

## CONCLUSIONS

A series of novel carbazole and triphenylamine-functionalized aromatic polyamides were readily prepared from the newly synthesized aromatic diamine monomer 4,4'-diamino-4''-(3,6-dimethoxycarbazol-9-yl)triphenylamine with various aromatic dicarboxylic acids via the phosphorylation polyamidation reaction. Because of the introduction of three-dimensional triphenylamine units and bulky 3,6-dimethoxycarbazole pendent groups in polymer backbone, all the polymers were amorphous, had good solubility in many polar aprotic solvents, and exhibited excellent film-forming ability. All the obtained polyamides revealed good electrochemical and electrochromic stability along with multielectrochromic behavior and enhanced NIR absorption upon oxidation. By substitution of the electrochemically active C-3 and C-6 sites of the carbazole unit with electron-donating methoxy groups, the new polyamides exhibit greatly enhanced electrochemical stability and electrochromic performance in comparison with previously reported analogs without methoxy substituents on the carbazole moiety. Such prominent features make these processable polymers amenable for optoelectronic applications such as OLEDs and electrochromic devices.

## ACKNOWLEDGMENT

The authors thank the National Science Council of Taiwan for the financial support.

## REFERENCES AND NOTES

- 1 P. M. S. Monk, R. J. Mortimer, D. R. Rosseinsky, *Electrochromism and Electrochromic Devices*; Cambridge University Press: Cambridge, UK, **2007**.
- 2 (a) D. R. Rosseinsky, R. J. Mortimer, *Adv. Mater.* **2001**, *13*, 783–793; (b) A. Michaelis, H. Berneth, D. Haarer, S. Kostromine, R. Neigl, R. Schmidt, *Adv. Mater.* **2001**, *13*, 1825–1828; (c) H. W. Heuer, R. Wehrmann, S. Kirchmeyer, *Adv. Funct. Mater.* **2002**, *12*, 89–94; (d) R. Baetens, B. P. Jelle, A. Gustavsen, *Sol. Energy Mater. Sol. Cells* **2010**, *94*, 87–105.
- 3 G. Sonmez, H. B. Sonmez, *J. Mater. Chem.* **2006**, *16*, 2473–2477.
- 4 (a) G. Sonmez, F. Wudl, *J. Mater. Chem.* **2005**, *15*, 20–22; (b) R. J. Mortimer, A. L. Dyer, J. R. Reynolds, *Displays* **2006**, *27*, 2–18; (c) P. Andersson, R. Forchheimer, P. Tehrani, M. Berggren, *Adv. Funct. Mater.* **2007**, *17*, 3074–3082; (d) F. C. Krebs, *Nat. Mater.* **2008**, *7*, 766–767.
- 5 (a) S. Beaupre, J. Dumas, M. Leclerc, *Chem. Mater.* **2006**, *18*, 4011–4018; (b) S. Beaupre, A.-C. Breton, J. Dumas, M. Leclerc, *Chem. Mater.* **2009**, *21*, 1504–1513.
- 6 (a) P. M. Beaujuge, J. R. Reynolds, *Chem. Rev.* **2010**, *110*, 268–320; (b) C. M. Amb, A. L. Dyer, J. R. Reynolds, *Chem. Mater.* **2011**, *23*, 397–415; (c) A. L. Dyer, E. J. Thompson, J. R. Reynolds, *ACS Appl. Mater. Interfaces* **2011**, *3*, 1787–1795; (d) A. Patra, M. Bendikov, *J. Mater. Chem.* **2010**, *20*, 422–433; (e) A. Balan, D. Baran, L. Toppare, *Polym. Chem.* **2011**, *2*, 1029–1043; (f) G. Gunbas, L. Toppare, *Chem. Commun.* **2012**, *48*, 1083–1101.
- 7 (a) L. Groenendaal, G. Zotti, P.-H. Aubert, S. M. Waybright, J. R. Reynolds, *Adv. Mater.* **2003**, *15*, 855–879; (b) J. Roncali, P. Blanchard, P. Frere, *J. Mater. Chem.* **2005**, *15*, 1589–1610; (c) S. Kirchmeyer, K. Reuter, *J. Mater. Chem.* **2005**, *15*, 2077–2088.
- 8 (a) C.-G. Wu, M.-I. Lu, S.-J. Chang, C.-S. Wei, *Adv. Funct. Mater.* **2007**, *17*, 1063–1070; (b) F. S. Han, M. Higuchi, D. G. Kurth, *J. Am. Chem. Soc.* **2008**, *130*, 2073–2081; (c) A. Maier, A. R. Rabindranath, B. Tieke, *Chem. Mater.* **2009**, *21*, 3668–3676; (d) M. A. Invernale, Y. Ding, D. M. D. Mamangun, M. S. Yavuz, G. A. Sotzing, *Adv. Mater.* **2010**, *22*, 1379–1382; (e) M. A. Invernale, Y. Ding, G. A. Sotzing, *ACS Appl. Mater. Interfaces* **2010**, *2*, 296–300; (f) M. I. Ozkut, S. Atak, A. M. Onal, A. Cihaner, *J. Mater. Chem.* **2011**, *21*, 5268–5272; (g) F. Baycan Koyuncu, E. Sefer, S. Koyuncu, E. Ozdemir, *Macromolecules* **2011**, *44*, 8407–8414.
- 9 (a) C. W. Tang, S. A. VanSlyke, *Appl. Phys. Lett.* **1987**, *51*, 913–915; (b) Y. Shirota, *J. Mater. Chem.* **2005**, *15*, 75–93; (c) Y. Shirota, H. Kageyama, *Chem. Rev.* **2007**, *107*, 953–1010.
- 10 (a) M.-Y. Chou, M.-k. Leung, Y. O. Su, C. L. Chiang, C.-C. Lin, J.-H. Liu, C.-K. Kuo, C.-Y. Mou, *Chem. Mater.* **2004**, *16*, 654–661; (b) L. Otero, L. Sereno, F. Fungo, Y.-L. Liao, C.-Y. Lin, K.-T. Wong, *Chem. Mater.* **2006**, *18*, 3495–3502; (c) B. Lim, Y.-C. Nah, J.-T. Hwang, J. Ghim, D. Vak, J.-M. Yun, D.-Y. Kim, *J. Mater. Chem.* **2009**, *19*, 2380–2385; (d) J. Natera, L. Otero, F. D'Eramo, L. Sereno, F. Fungo, N.-S. Wang, Y.-M. Tsai, K.-T. Wong, *Macromolecules* **2009**, *42*, 626–635; (e) H.-Y. Wu, K.-L. Wang, D.-J. Liaw, K.-R. Lee, J.-Y. Lai, *J. Polym. Sci. Part A: Polym. Chem.* **2010**, *48*, 1469–1476; (f) H.-J. Yen, G.-S. Liou, *Polym. Chem.* **2012**, *3*, 255–264.
- 11 M. Thelakkat, *Macromol. Mater. Eng.* **2002**, *287*, 442–461.
- 12 (a) E. T. Seo, R. F. Nelson, J. M. Fritsch, L. S. Marcoux, D. W. Leedy, R. N. Adams, *J. Am. Chem. Soc.* **1966**, *88*, 3498–3503; (b) R. F. Nelson, R. N. Adams, *J. Am. Chem. Soc.* **1968**, *90*, 3925–3930.
- 13 (a) S.-H. Cheng, S.-H. Hsiao, T.-H. Su, G.-S. Liou, *Macromolecules* **2005**, *38*, 307–316; (b) G.-S. Liou, S.-H. Hsiao, H.-W. Chen, *J. Mater. Chem.* **2006**, *16*, 1831–1842; (c) S.-H. Hsiao, G.-S. Liou, Y.-C. Kung, H.-J. Yen, *Macromolecules* **2008**, *41*, 2800–2808; (d) Y.-C. Kung, G.-S. Liou, S.-H. Hsiao, *J. Polym. Sci. Part A: Polym. Chem.* **2009**, *47*, 1740–1755; (e) S.-H. Hsiao, G.-S. Liou, Y.-C. Kung, H.-Y. Pan, C.-H. Kuo, *Eur. Polym. J.* **2009**, *45*, 2234–2248; (f) Y.-C. Kung, S.-H. Hsiao, *J. Mater. Chem.* **2011**, *21*, 1746–1754; (g) Y.-C. Kung, W.-F. Lee, S.-H. Hsiao, G.-S. Liou, *J. Polym. Sci. Part A: Polym. Chem.* **2011**, *49*, 2210–2221; (h) Y.-C. Kung, S.-H. Hsiao, *J. Polym. Sci. Part A: Polym. Chem.* **2011**, *49*, 3475–3490.
- 14 J. M. Garcia, F. C. Garcia, F. Serna, J. L. de la Pena, *Prog. Polym. Sci.* **2010**, *35*, 623–686.
- 15 (a) S.-H. Hsiao, Y.-M. Chang, H.-W. Chen, G.-S. Liou, *J. Polym. Sci. Part A: Polym. Chem.* **2006**, *44*, 4579–4592; (b) C.-W. Chang, G.-S. Liou, S.-H. Hsiao, *J. Mater. Chem.* **2007**, *17*, 1007–1015; (c) S.-H. Hsiao, G.-S. Liou, Y.-C. Kung, Y.-M. Chang, *J. Polym. Sci. Part A: Polym. Chem.* **2010**, *48*, 2798–2809.
- 16 (a) M.-H. Tsai, T.-H. Ke, H.-W. Lin, C.-C. Wu, S.-F. Chiu, F.-C. Fang, Y.-L. Liao, K.-T. Wong, Y.-H. Chen, C.-I. Wu, *ACS Appl. Mater. Interfaces* **2009**, *1*, 567–574; (b) Y.-T. Tao, Q. Wang, C.-L. Yang, C. Zhong, K. Zhang, J.-G. Qin, D.-G. Ma, *Adv. Funct. Mater.* **2010**, *20*, 304–311; (c) W. Jiang, L. Duan, J. Qiao, G. F. Dong, D.-Q. Zhang, L.-D. Wang, Y. Qiu, *J. Mater. Chem.* **2011**, *21*, 4918–4926; (d) L.-X. Xiao, Z.-J. Chen, B. Qu, J.-X. Luo, S. Kong, Q.-H. Gong, J. Kido, *Adv. Mater.* **2011**, *23*, 926–952; (e) Y.-T. Tao, C.-L. Yang, J.-G. Qin, *Chem. Soc. Rev.* **2011**, *40*, 2943–2970.
- 17 J. P. Chen, A. Natansohn, *Macromolecules* **1999**, *32*, 3171–3177.
- 18 (a) J. V. Grazulevicius, P. Strohmriegl, J. Pielichowski, K. Pielichowski, *Prog. Polym. Sci.* **2003**, *28*, 1297–1353; (b) J.-F. Morin, M. Leclerc, D. Ades, A. Siove, *Macromol. Rapid Commun.* **2005**, *26*, 761–778; (c) S. Walkim, B.-R. Aich, Y. Tao, M. Leclerc, *Polym. Rev.* **2008**, *48*, 432–462; (d) N. Blouin, M.

- Leclerc, *Acc. Chem. Res.* **2008**, *41*, 1110–1119; (e) P.-L. T. Boudreault, S. Beaupre, M. Leclerc, *Polym. Chem.* **2010**, *1*, 127–136.
- 19** G.-S. Liou, H.-W. Chen, H.-J. Yen, *J. Polym. Sci. Part A: Polym. Chem.* **2006**, *44*, 4108–4121.
- 20** J. Huang, Y. H. Niu, W. Yang, Y. Q. Mo, M. Yuan, Y. Cao, *Macromolecules* **2002**, *35*, 6080–6082.
- 21** Y. Kikugawa, Y. Aoki, T. Sakamoto, *J. Org. Chem.* **2001**, *66*, 8612–8615.
- 22** N. Yamazaki, M. Matsumoto, F. Higashi, *J. Polym. Sci. Polym. Chem. Ed.* **1975**, *13*, 1375–1380.
- 23** (a) J. F. Ambrose, R. F. Nelson, *J. Electrochem. Soc.* **1968**, *115*, 1159–1164; (b) J. F. Ambrose, L. L. Carpenter, R. F. Nelson, *J. Electrochem. Soc.* **1975**, *122*, 876–894.
- 24** (a) C. Lambert, G. Noll, *J. Am. Chem. Soc.* **1999**, *121*, 8434–8442; (b) A. V. Azeghalmi, M. Erdmann, V. Kriegisch, G. Noll, R. Stahl, C. Lambert, D. Leusser, D. Stalke, M. Zabel, J. Popp, *J. Am. Chem. Soc.* **2004**, *126*, 7834–7845.